Applied Mathematics, 2011, 2, 414-423
doi:10.4236/am.2011.24051 Published Online April 2011 (http://www.SciRP.org/journal/am)

RBFs Meshless Method of Lines for the Numerical Solution of Time-Dependent Nonlinear Coupled Partial Differential Equations

Sirajul Haq[1], Arshad Hussain[1], Marjan Uddin[2,3*]
[1]*Faculty of Engineering Sciences, Ghulam Ishaq Khan Institute of Engineering Sciences and Technology, Topi, Pakistan*
[2]*Department of Applied Mathematics, Illinois Institute of Technology, Chicago, USA*
[3]*Department of Mathematics, Karakoram International University, Gilgit, Pakistan*
*E-mail: siraj_jcs@yahoo.co.in, math_pal@hotmail.com, marjankhan1@hotmail.com**
Received December 25, 2010; *revised February* 3, 2011; *accepted February* 6, 2011

Abstract

In this paper a meshless method of lines is proposed for the numerical solution of time-dependent nonlinear coupled partial differential equations. Contrary to mesh oriented methods of lines using the finite-difference and finite element methods to approximate spatial derivatives, this new technique does not require a mesh in the problem domain, and a set of scattered nodes provided by initial data is required for the solution of the problem using some radial basis functions. Accuracy of the method is assessed in terms of the error norms L_2, L_∞ and the three invariants C_1, C_2, C_3. Numerical experiments are performed to demonstrate the accuracy and easy implementation of this method for the three classes of time-dependent nonlinear coupled partial differential equations.

Keywords: RBFs, Meshless Method of Lines, Time-Dependent PDEs

1. Introduction

Nonlinear coupled partial differential equations have numerous applications in the field of science and engineering, including solid state physics, fluid mechanics, chemical physics, plasma physics etc. (see [1-3] and the references therein). In 1981 Hirota-Satsuma introduced the coupled KdV equations, [4] which has many applications in physical sciences. Coupled KdV equations describe an interaction of the two long waves with different dispersion relation. The Burgers' equations describe phenomena such as a mathematical model of turbulence [5] and the nonlinear hyperbolic system [6] represents interaction of the two waves traveling in the opposite directions.

In the last decade many authors have studied the numerical and approximate solution of time-dependent nonlinear coupled partial differential equations by various numerical methods. These include Adomian decomposition method [7], the local discontinuous Galerkin method [8], the variational iteration method [9], the Chebyshev spectral collocation method [10] and the radial basis functions method [6,11,12].

In the last decade, the theory of radial basis functions (RBFs) has enjoyed a great success as scattered data interpolating technique. A radial basis function, $\phi(x-x_j)=\phi(\|x-x_j\|)$, is a continuous spline which depends upon the separation distances of a subset of data centers, $X\subset\Re^n$, $\{x_j\in X, j=1,2,\cdots,N\}$. Due to spherical symmetry about the centers x_j, the RBFs are called radial. The distances, $\|x-x_j\|$, are usually taken to be the Euclidean metric.

Hardy [13] was the first to introduced a general scattered data interpolation method, called radial basis functions method for the approximation of two-dimensional geographical surfaces. In 1982 Franke [14] in a review paper made the comparison among all the interpolation methods for scattered data sets available at that time, and the radial basis functions outperformed all the other methods regarding efficiency, stability and ease of implementations. Franke found that Hardy's multiquadrics (MQ) were ranked the best in accuracy, followed by thin plate splines (TPS). Despite MQ's excellent performance, it contains a shape parameter c, and the accuracy of MQ is greatly affected by the choice of shape parameter c whose optimal value is still unknown. Franke [15] used the formula $c^2=(1.25)^2 d^2$ where d is the mean distance from each data point to its nearest neighbor. Hickernell and Hon [16] and Golberg *et al.* [17] had successfully used the technique of cross-validation to obtain an optimal value of the shape parameter. Various researchers have contributed recently to this field (see [18-25] ect.)

The method of lines (MOL) [26] is a general procedure for the solution of time dependent partial differential equations (PDEs). The basic idea of the MOL is to replace the spatial (boundary value) derivatives in the PDEs with algebraic approximations. Once this is done, the spatial derivatives are no longer stated explicitly in terms of the spatial independent variables. Thus only the initial value variable, typically time in a physical problem, remains. In other words, we have a system of ODEs that approximate the original PDE. Now we can apply any integration algorithm for initial value ODEs to compute an approximate numerical solution to the PDE. Thus, one of the salient features of the MOL is the use of existing, and generally well established, numerical methods for ODEs. Very recently Quan Shen [27] use this approach for the numerical solution of KdV equation. In this paper, we will use RBFs approximation method with the method of lines (MOL) for the numerical solution of time-dependent nonlinear partial differential equations given as:

Class A: Coupled KdV equations

$$u_t = -\alpha u_{xxx} - 6\alpha u u_x + 2\nu v v_x,$$

$$v_t = -\beta v_{xxx} - 3\beta u v_x,$$

Class B: Coupled Burgers' equations

$$u_t = u_{xx} - 2uu_x - \alpha(uv)_x,$$

$$v_t = v_{xx} - 2vv_x - \beta(uv)_x,$$

Class C: System of nonlinear hyperbolic equations

$$u_t = -u_x - \alpha uv,$$

$$v_t = v_x - \alpha uv,$$

where α, β, ν are positive parameters.

Rest of the paper is organized as follows: In Section 2, The radial basis functions collocation method coupled with MOL is presented. Section 3 is devoted to the numerical tests of the method on the problems related to the coupled KdV, the coupled Burgers' equations and the system of nonlinear hyperbolic equations. In Section 4, the results are concluded.

2. RBFs Meshless Method of Lines

2.1. Coupled KdV Equations

Consider the nonlinear coupled KdV equations,

$$\begin{aligned} u_t &= -\alpha u_{xxx} - 6\alpha u u_x + 2\nu v v_x, \\ v_t &= -\beta v_{xxx} - 3\beta u v_x, \end{aligned} \tag{1}$$

with boundary conditions

$$\begin{aligned} u(a,t) &= f_1(t),\ u(b,t) = f_2(t), \\ v(a,t) &= g_1(t),\ v(b,t) = g_2(t),\ t > 0, \end{aligned} \tag{2}$$

and initial conditions

$$\begin{aligned} u(x,0) &= f(x), \\ v(x,0) &= g(x),\ a \le x \le b, \end{aligned} \tag{3}$$

where α, β, ν are positive real constants.

For a given set of N collocation points $\{x_i\}_{i=1}^N$ in the domain $[a,b]$, the RBFs approximation for u and v of (1) are given by

$$U(x) = \sum_{j=1}^{N} \lambda_1 \phi_j(r),\ V(x) = \sum_{j=1}^{N} \lambda_2 \phi_j(r), \tag{4}$$

where $\{\lambda_j\}_{j=1}^N$ are the unknown constants to be determined, $\phi_j(r) = \phi(\|x - x_j\|)$ can be any well known radial basis function and $r_j = \|x - x_j\|$ is the Euclidean norm between points x and x_j. Here we are using two radial basis functions, the multiquadric $\phi(r) = \sqrt{r^2 + c^2}$ and cubic $\phi(r) = r^3$. Now for each node x_i, $i = 1,2,3,\cdots,N$ in the domain $[a,b]$, (4) can be written as

$$\boldsymbol{U} = \boldsymbol{A}\boldsymbol{\lambda}_1, \boldsymbol{V} = \boldsymbol{A}\boldsymbol{\lambda}_2, \tag{5}$$

where

$$\boldsymbol{U} = [U(x_1), U(x_2), U(x_3), \cdots, U(x_N)]^T$$

$$\boldsymbol{\lambda_i} = [\lambda_{i1}, \lambda_{i2}, \lambda_{i3}, \cdots, \lambda_{iN}]^T,\ i = 1,2.$$

$$\boldsymbol{A} = \begin{bmatrix} \Phi^T(x_1) \\ \Phi^T(x_1) \\ \cdots \\ \Phi^T(x_N) \end{bmatrix} = \begin{bmatrix} \phi_1(x_1) & \phi_2(x_1) & \cdots & \phi_N(x_1) \\ \phi_1(x_2) & \phi_1(x_2) & \cdots & \cdots \\ \vdots & \vdots & \ddots & \vdots \\ \phi_1(x_N) & \phi_1(x_N) & \cdots & \phi_N(x_N) \end{bmatrix}$$

$$\Phi^T(x_i) = [\phi_1(x_i), \phi_2(x_i), \phi_3(x_i), \cdots, \phi_N(x_i)],$$

where $i = 1,2,3,\cdots,N$.

Equation (4) can also be written as

$$\begin{aligned} U(x) &= \Phi^T(x)\boldsymbol{A}^{-1}\boldsymbol{U} = \boldsymbol{D}(\boldsymbol{x})\boldsymbol{U}, \\ V(x) &= \Phi^T(x)\boldsymbol{A}^{-1}\boldsymbol{V} = \boldsymbol{D}(\boldsymbol{x})\boldsymbol{V} \end{aligned} \tag{6}$$

where

$$\boldsymbol{D}(\boldsymbol{x}) = \Phi^T(x)\boldsymbol{A}^{-1} = [D_1(x), D_2(x), \cdots, D_N(x)].$$

Using the approximations $U_i(t)$ and $V_i(t)$ of the solutions $u(x_i,t)$ and $v(x_i,t)$ given in (6), (1) at each node x_i, $i=1,2,3,\cdots,N$ can be written as

$$\frac{\mathrm{d}U_i}{\mathrm{d}t} = -\alpha D_{xxx}(x_i)\boldsymbol{U} - 6\alpha U_i\left(D_x(x_i)\boldsymbol{U}\right)\mathbb{F} + 2\nu V_i\left(D_x(x_i)\boldsymbol{V}\right) \tag{7}$$

$$\frac{\mathrm{d}V_i}{\mathrm{d}t} = -\beta D_{xxx}(x_i)\boldsymbol{V} - 3\beta U_i\left(D_x(x_i)\boldsymbol{V}\right)$$

where

$$\boldsymbol{D_x}(\boldsymbol{x}_i) = \left[D_{1x}(x_i), D_{2x}(x_i), \cdots, D_{Nx}(x_i)\right],$$

$$D_{jx}(x_i) = \frac{\partial}{\partial x}D_j(x_i), \quad j=1,2,\cdots,N,$$

$$\boldsymbol{D_{xxx}}(\boldsymbol{x}_i) = \left[D_{1xxx}(x_i), D_{2xxx}(x_i), \cdots, D_{Nxxx}(x_i)\right]$$

$$D_{jxxx}(x_i) = \frac{\partial^3}{\partial x^3}D_j(x_i), \quad j=1,2,\cdots,N.$$

In more compact form (7) can be written as

$$\begin{aligned}\frac{\mathrm{d}\boldsymbol{U}}{\mathrm{d}t} &= -\alpha\boldsymbol{D}_{xxx}\boldsymbol{U} - 6\alpha\boldsymbol{U}*\left(\boldsymbol{D}_x\boldsymbol{U}\right) + 2\nu\boldsymbol{V}*\left(\boldsymbol{D}_x\boldsymbol{V}\right),\\ \frac{\mathrm{d}\boldsymbol{V}}{\mathrm{d}t} &= -\beta\boldsymbol{D}_{xxx}\boldsymbol{V} - 3\beta\boldsymbol{U}*\left(\boldsymbol{D}_x\boldsymbol{V}\right),\end{aligned} \tag{8}$$

where the symbol * denotes component by component multiplication of two vectors and

$$\boldsymbol{D}_x = \left[D_{jx}(x_i)\right]_{i,j=1}^{N}, \quad \boldsymbol{D}_{xxx} = \left[D_{jxxx}(x_i)\right]_{i,j=1}^{N}.$$

For simplicity we write (8) as

$$\frac{\mathrm{d}\boldsymbol{U}}{\mathrm{d}t} = F_1(\boldsymbol{U},\boldsymbol{V}), \quad \frac{\mathrm{d}\boldsymbol{V}}{\mathrm{d}t} = F_2(\boldsymbol{U},\boldsymbol{V}), \tag{9}$$

where

$$F_1(\boldsymbol{U},\boldsymbol{V}) = -\alpha\boldsymbol{D}_{xxx}\boldsymbol{U} - 6\alpha\boldsymbol{U}*\left(\boldsymbol{D}_x\boldsymbol{U}\right) + 2\nu\boldsymbol{V}*\left(\boldsymbol{D}_x\boldsymbol{V}\right),$$

$$F_2(\boldsymbol{U},\boldsymbol{V}) = -\beta\boldsymbol{D}_{xxx}\boldsymbol{V} - 3\beta\boldsymbol{U}*\left(\boldsymbol{D}_x\boldsymbol{V}\right).$$

The corresponding boundary conditions are given by

$$\begin{aligned}U_1 &= f_1(t), \quad U_N = f_2(t)\\ V_1 &= g_1(t), \quad V_N = g_2(t),\end{aligned} \tag{10}$$

and the initial conditions are as

$$\begin{aligned}\boldsymbol{U}(t_0) &= \left[f(x_1), f(x_2), \cdots, f(x_N)\right]\\ \boldsymbol{V}(t_0) &= \left[g(x_1), g(x_2), \cdots, g(x_N)\right]\end{aligned} \tag{11}$$

Now we solve the system of ODEs (9)-(11) by using the well known ODE solvers.

1) The classical forth order Runge-Kutta method (RK4) given by

$$\boldsymbol{U}^{n+1} = \boldsymbol{U}^n + \frac{\delta t}{6}\left(K_1 + 2K_2 + 2K_3 + K_4\right),$$

$$\boldsymbol{V}^{n+1} = \boldsymbol{V}^n + \frac{\delta t}{6}\left(J_1 + 2J_2 + 2J_3 + J_4\right),$$

where

$$K_1 = F_1\left(\boldsymbol{U}^n, \boldsymbol{V}^n\right), \quad K_2 = F_1\left(\boldsymbol{U}^n + \delta t K_1/2, \boldsymbol{V}^n\right),$$

$$K_3 = F_1\left(\boldsymbol{U}^n + \delta t K_2/2, \boldsymbol{V}^n\right), \quad K_4 = F_1\left(\boldsymbol{U}^n + \delta t K_3, \boldsymbol{V}^n\right),$$

$$J_1 = F_2\left(\boldsymbol{U}^n, \boldsymbol{V}^n\right), \quad J_2 = F_2\left(\boldsymbol{U}^n, \boldsymbol{V}^n + \delta t J_1/2\right),$$

$$J_3 = F_2\left(\boldsymbol{U}^n, \boldsymbol{V}^n + \delta t J_2/2\right), \quad J_4 = F_2\left(\boldsymbol{U}^n, \boldsymbol{V}^n + \delta t J_3\right),$$

2) Low-storage third-order (TVD-RK3) scheme given by [28]

$$\boldsymbol{U}^{(1)} = \boldsymbol{U}^n + \delta t F_1\left(\boldsymbol{U}^n, \boldsymbol{V}^n\right),$$

$$\boldsymbol{U}^{(2)} = \frac{3}{4}\boldsymbol{U}^n + \frac{1}{4}\boldsymbol{U}^{(1)} + \frac{1}{4}\delta t F_1\left(\boldsymbol{U}^{(1)}, \boldsymbol{V}^n\right),$$

$$\boldsymbol{U}^{(n+1)} = \frac{1}{3}\boldsymbol{U}^n + \frac{2}{3}\boldsymbol{U}^{(2)} + \frac{2}{3}\delta t F_1\left(\boldsymbol{U}^{(2)}, \boldsymbol{V}^n\right),$$

$$\boldsymbol{V}^{(1)} = \boldsymbol{V}^n + \delta t F_2\left(\boldsymbol{U}^n, \boldsymbol{V}^n\right),$$

$$\boldsymbol{V}^{(2)} = \frac{3}{4}\boldsymbol{V}^n + \frac{1}{4}\boldsymbol{V}^{(1)} + \frac{1}{4}\delta t F_2\left(\boldsymbol{U}^n, \boldsymbol{V}^{(1)}\right),$$

$$\boldsymbol{V}^{(n+1)} = \frac{1}{3}\boldsymbol{V}^n + \frac{2}{3}\boldsymbol{V}^{(2)} + \frac{2}{3}\delta t F_2\left(\boldsymbol{U}^n, \boldsymbol{V}^{(2)}\right).$$

2.2. Nonlinear Coupled Burgers' Equations

Consider the nonlinear coupled Burgers' equations

$$\begin{aligned}u_t &= u_{xx} - 2uu_x - \alpha(uv)_x,\\ v_t &= v_{xx} - 2vv_x - \beta(uv)_x,\end{aligned} \tag{12}$$

with the boundary conditions

$$\begin{aligned}u(a,t) &= f_1(t), \; u(b,t) = f_2(t),\\ v(a,t) &= g_1(t), \; v(b,t) = g_2(t), \; t>0,\end{aligned} \tag{13}$$

and initial conditions

$$\begin{aligned}u(x,0) &= f(x),\\ v(x,0) &= g(x), \; a \le x \le b,\end{aligned} \tag{14}$$

where α,β,ν are positive parameters. The same procedure as discussed in Section 2.1 can be used for the solution of (12)-(14).

2.3. Nonlinear Coupled Hyperbolics

Consider the nonlinear hyperbolic system

$$u_t = -u_x - \alpha uv, \quad v_t = v_x - \alpha uv, \tag{15}$$

with boundary conditions

$$u(a,t)=f_1(t),\ u(b,t)=f_2(t),$$
$$v(a,t)=g_1(t),\ \ v(b,t)=g_2(t),\ \ t>0, \tag{16}$$

and initial conditions

$$u(x,0)=f(x),$$
$$v(x,0)=g(x),\ \ a\le x\le b, \tag{17}$$

where α is a positive real constant. The same procedure as discussed in Section 2.1 can be used for the solution of (15)-(17).

3. Numerical Examples

In this section, we apply the RBFs meshless method of lines for the numerical solution of three classes of partial differential equations, defined earlier. We use the L_2 and L_∞ error norms to measure the difference between the numerical and analytic solutions. The L_2 and L_∞ error norms of the solution are defined by

$$L_2=\|u-U\|_2=\left[\delta x\sum_{j=1}^{N}(u-U)^2\right]^{1/2},$$
$$L_\infty=\|u-U\|_\infty=\max_j|u-U|, \tag{18}$$

We examine our results by calculating the following three conservative laws. Hirota-Satsuma [4] proved that the coupled KdV equations defined in (1) possesses three conserved quantities for all values of $\alpha=\beta$ and ν.

$$C_1=\int_a^b u\,\mathrm{d}x,$$
$$C_2=\int_a^b\left(u^2+\frac{2}{3}\nu v^2\right)\mathrm{d}x \tag{19}$$
$$C_3=\int_a^b\left[(1+a)\left(u^3-\frac{1}{2}(u_x)^2\right)+\nu\left(uv^2-(v_x)^2\right)\right]\mathrm{d}x.$$

Later Hirota-Satsuma [29] showed that the system (7) has infinitely many conserved quantities for the choice of $\alpha=1/2$ and arbitrary values of β and ν. In our investigation we consider the conserved quantities C_1, C_2 and C_3 only. In this section, we apply meshless MOL using radial basis functions on the three classes of partial differential equations defined earlier.

Problem 1 We consider the nonlinear coupled KdV Equations (1) for $\nu = 3$ $\alpha=\beta$ and with exact solution [20]

$$u(x,t)=\frac{\lambda}{\alpha}\sec h^2\left[\frac{1}{2}\sqrt{\frac{\lambda}{\alpha}}(x-\lambda t)\right],$$
$$v(x,t)=\frac{\lambda}{\sqrt{2\alpha}}\sec h^2\left[\frac{1}{2}\sqrt{\frac{\lambda}{\alpha}}(x-\lambda t)\right]. \tag{20}$$

where α,β are arbitrary constants. The boundary conditions $u(a,t)$, $u(b,t)$, $v(a,t)$ and $v(b,t)$ and the initial conditions $u(x,0),v(x,0)$ are extracted from the exact solution (20). We solved the problem in the spatial interval $-5\le x\le 5$ by RBFs meshless method of lines using RK4 and TVD-RK3 time integration schemes. In our computations we used multiquadric (MQ) radial basis function. The results are presented in **Tables 1-4**, and in **Figure 1**. It is observed that the two schemes RK4 and TVD-RK3 show same order of accuracy, but TVD-RK3 scheme is more faster than RK4 scheme, and both remained stable for small time step size δt It is also observed that the three invariants C_1, C_2 and C_3 as well as their normalized values,

$$NC_1=(C_1(t)-C_1(0))/C_1(0),$$
$$NC_2=(C_2(t)-C_2(0))/C_2(0),$$
$$NC_3=(C_3(t)-C_3(0))/C_3(0),$$

are absolutely conserved in time during the computations which demonstrates the accuracy of the schemes. We also noted that the value of MQ shape parameter for which the solution converges belongs to the interval $0.1\le c\le 0.6$ as shown in **Table 3**. The motion of solitary waves u and v is shown in **Figure 1**, which are initially centered at $x=0$ moving from left to right with the constant speed λ, having the amplitudes λ/α and $\lambda/\sqrt{2\alpha}$ respectively.

Problem 2 Consider the nonlinear coupled Burgers' Equations (12), whose exact solution [10] is given by

$$u(x,t)=a_0-2A\left(\frac{2\alpha-1}{4\alpha\beta-1}\right)\tanh\left[A(x-2At)\right],$$
$$v(x,t)=a_0\left(\frac{2\beta-1}{2\alpha-1}\right)-2A\left(\frac{2\alpha-1}{4\alpha\beta-1}\right)\tanh\left[A(x-2At)\right]. \tag{21}$$

where $A=(1/2)(a_0(4\alpha\beta-1))/(2\alpha-1)$, a_0, α, β are arbitrary constants.

The boundary conditions $u(a,t)$, $u(b,t)$, $v(a,t)$, $v(b,t)$ and the initial conditions $u(x,0)$, $v(x,0)$ are extracted from the exact solution (21). We solved the problem in the domain $-10\le x\le 10$ by using MOL coupled with RBFs collocation method. The classical RK4 and TVD-RK3 scheme are used in our computations. The results are listed in **Table 5** and **Figure 2**, and compare with earlier results [10]. It is observed that the results are comparable with [10] and well agreed with the exact solution.

Problem 3 Now we consider nonlinear coupled hyperbolic Equations (15). For the sake of comparison [6], we take $a=-0.5$, $b=0.5$, $\nu=100$ and the initial conditions.

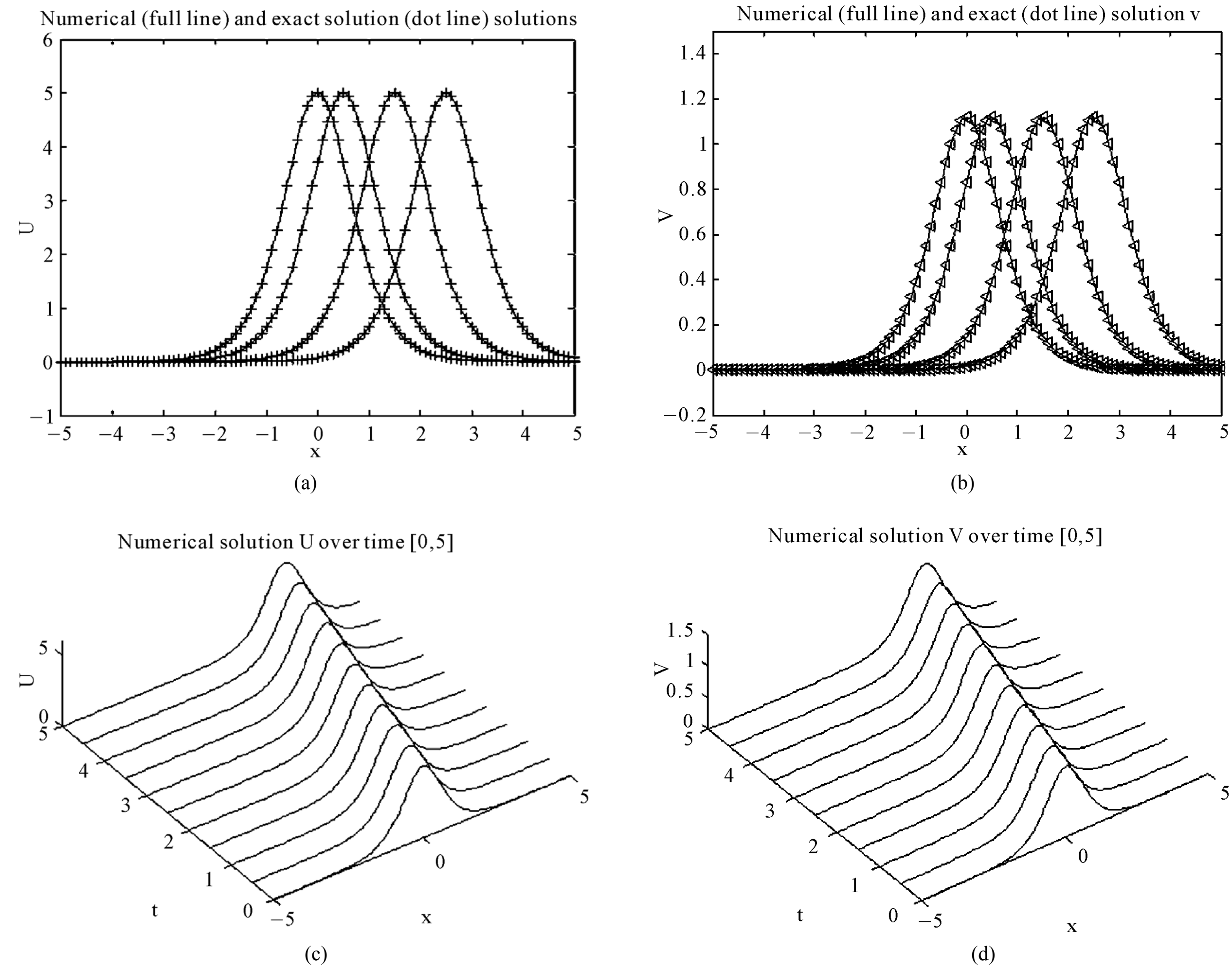

Figure 1. Plots of Problem 1 corresponding to α = 0.1, β = 0.1, λ = 0.5, δ_x = 0.1, δ_t = 0.001, c = 0.58. Figures 1(a) and 1(b) show the motion of the solitary waves u and v moving from left to right, initially centered at x = 0 when t = 0,1,2,3,4,5. Figures 1(c) and 1(d) represent numerical solutions u and v over time [0,5].

$$u(x,0)=\begin{cases}0.5\left[1+\cos(10\pi x)\right], & x\in[-0.3,-0.1];\\ 0, & \text{otherwise}\end{cases} \tag{22}$$

$$v(x,0)=\begin{cases}0.5\left[1+\cos(10\pi x)\right], & x\in[0.1,0.3];\\ 0, & \text{otherwise}\end{cases} \tag{23}$$

and the boundary conditions

$$\begin{aligned} u(a,t)&=u(b,t)=0,\\ v(a,t)&=v(b,t)=0. \end{aligned} \tag{24}$$

This problem is solved by RBFs meshless method of lines using MQ with RK4 scheme. We take the initial solutions v and $v(x,0)$ which are located at $x=-0.2$ and $x=0.2$, respectively. When $t>0$ the nonlinear term, uv, causes these waves to move without change in shape, u to the right and v to the left. The two waves collide when $t=0.1$ which results in change of shapes of the waves. The two waves overlap each other near $t=0.25$ and they separate again at $t=0.3$ approximately. From this time onwards the linear term becomes dominant and the pulses lose their symmetry and experience a decrease in the amplitude due to nonlinear interaction as shown in the **Figures 3(a)-3(f)**. The numerical results of the solutions u and v are presented graphically. Since the exact solution of this problem is not known, we use cubic radial basis function r^3 to find the numerical solution. These graphical results are agreed well with the results obtained by quasi-linear interpolation method [6].

4. Closure

We have applied the meshless method of lines using radial basis functions for the numerical solutions of time-dependent nonlinear coupled partial differential equa-

Table 1. Error norms and the three invariants for the solutions u, v using MQ when δ_t = 0.001, N = 100 c = 0.53. α = 0.01, β = 0.01 and λ = 0.01 corresponding to Problem 1.

t	$L_\infty(u)$	$L_2(u)$	$L_\infty(v)$	$L_2(v)$	C_1	C_2	C_3
RK4							
0.1	9.625E–05	3.676E–05	6.807E–06	2.601E–06	3.94906	2.69268	1.90965
1	3.368E–05	3.990E–05	2.373E–06	2.829E–06	3.94906	2.69268	1.90965
5	1.040E–04	1.471E–04	7.392E–06	1.040E–05	3.94896	2.69268	1.90966
10	2.514E–04	4.711E–04	1.791E–05	3.323E–05	3.94867	2.69267	1.90967
15	4.427E–04	1.003E–03	3.141E–05	7.109E–05	3.94819	2.69265	1.90968
20	6.962E–04	1.681E–03	4.916E–05	1.190E–04	3.94754	2.69261	1.90969
TVD-RK3							
0.1	9.627E–05	3.676E–05	6.807E–06	2.601E–06	3.94906	2.69268	1.90965
1	3.353E–05	3.977E–05	2.373E–06	2.831E–06	3.94906	2.69268	1.90965
5	1.046E–04	1.459E–04	7.392E–06	1.041–05	3.94896	2.69267	1.90965
10	2.535E–04	4.675E–04	1.791E–05	3.326E–05	3.94867	2.69266	1.90965
15	4.446E–04	1.003E–03	3.141E–05	7.117E–05	3.94819	2.69263	1.90965
20	6.952E–04	1.679E–03	4.916E–05	1.191E–04	3.94754	2.69258	1.90965

Table 2. The three invariants and its normalized invariants for the solutions u, v using MQ, when, δ_t = 0.001, N = 100, c_1 = 0.53, c_2 = 0.53, α = 0.05, β = 0.05, λ = 0.05 corresponding to Problem 1.

t	C_1	C_2	C_3	NC_1	NC_2	NC_3	Amp(u)	Amp(v)
RK4								
0.1	3.94906	2.79932	2.08037	1.248E–07	1.199E–08	4.186E–08	1.000	0.158
0.3	3.94905	2.79932	2.08037	1.570E–06	6.969E–07	2.310E–06	1.000	0.158
0.5	3.94903	2.79933	2.08038	6.670E–06	1.119E–06	3.999E–06	1.000	0.158
1	3.94896	2.79933	2.08039	2.409E–05	1.745E–06	8.336E–06	0.999	0.158
3	3.94819	2.79930	2.08043	2.195E–04	7.809E–06	2.828E–05	0.999	0.158
5	3.94671	2.79922	2.08046	5.954E–04	3.697E–05	4.491E–05	1.000	0.158

Table 3. Error norms and normalized invariants of the solutions u, v for different values of MQ shape parameter c when t = 1.0, δ_t = 0.001, N = 100, α = 0.1, β = 0.1, λ = 0.5 corresponding to Problem 1.

c	$L_\infty(u)$	$L_\infty(v)$	NC_1	NC_2	NC_3
RK4					
0.1	1.492E–01	3.101E–02	9.986E–05	3.112E–04	3.956E–03
0.2	8.632E–03	5.410E–04	2.656E–05	3.201E–04	7.502E–04
0.3	7.789E–03	4.934E–04	1.598E–05	3.202E–04	7.240E–04
0.4	7.795E–03	4.960E–04	9.505E–06	3.202E–04	7.239E–04
0.5	7.785E–03	4.944E–04	6.102E–06	3.202E–04	7.240E–04
0.6	7.816E–03	4.846E–04	7.137E–06	3.200E–004	7.236E–04

Table 4. Error norms and normalized invariants of the solutions *u*, *v* for different values of time step size δ_t when $t = 1.0$, $c = 0.53$, $N = 100$, $\alpha = 0.1$, $\beta = 0.1$, $\lambda = 0.5$ corresponding to Problem 1.

δt	$L_\infty(u)$	$L_\infty(v)$	NC_1	NC_2	NC_3
RK4					
0.001	7.804E–03	4.932E–04	5.485E–06	3.203E–04	7.241E–04
0.0005	3.880E–03	2.458E–04	4.615E–06	9.281E–05	2.108E–04
0.0001	7.774E–04	6.294E–05	3.709E–06	8.735E–05	1.956E–04
0.00005	3.919E–04	6.257E–05	3.817E–06	1.098E–04	2.461E–04
0.00001	2.779E–04	6.230E–05	3.745E–06	1.277E–04	2.865E–04

Table 5. Error norms of solutions *u* and *v* v using MQ, corresponding to Problem 2.

										L_∞		
	t	δt	δx	α	β	a	b	a_0	c	RK4	TVD-RK3	ChSC[10]
U	0.5	0.001	0.25	0.1	0.3	–10	10	0.05	0.58	4.169E–05	4.169E–05	4.16E–05
	1.0									8.243E–05	8.243E–05	8.23E–05
	0.5	0.001	0.25	0.3	0.03	–10	10	0.05	0.58	4.591E–05	4.591E–05	4.59E–05
	1.0									9.183E–05	9.183E–05	9.16E–05
V	0.5	0.001	0.25	0.1	0.3	–10	10	0.05	0.58	2.157E–05	2.157E–05	2.19E–05
	1.0									4.166E–05	4.166E–05	4.10E–05
	0.5	0.001	0.25	0.3	0.03	–10	10	0.05	0.58	1.809E–04	1.809E–04	1.80E–04
	1.0									3.617E–04	3.617E–04	3.59E–04

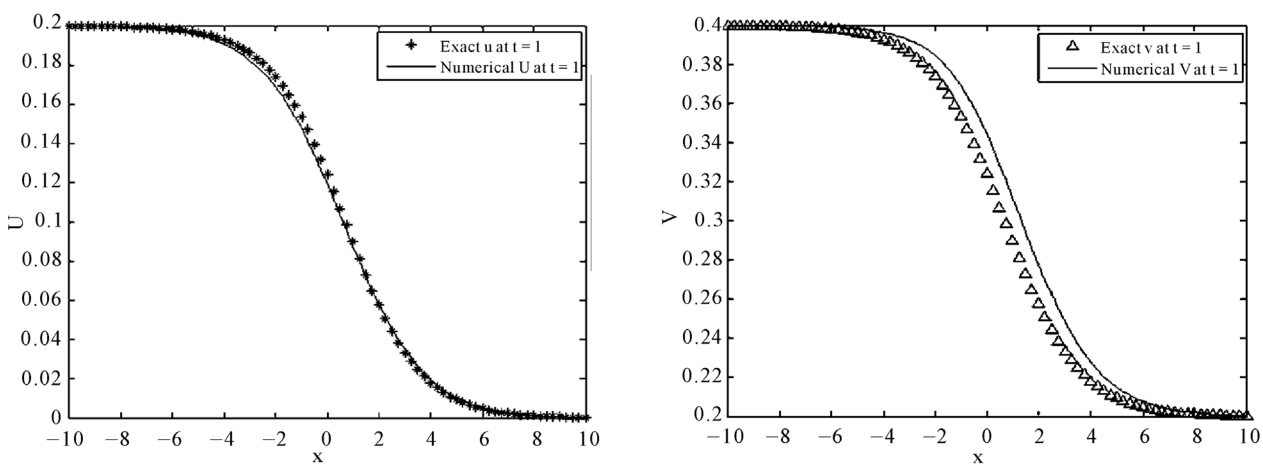

(a) (b)

Figure 2. Comparison of numerical solution using RK4 with MQ versus exact solutions *u*, *v* at time $t = 1$ when $\alpha = 1$, $\beta = 2$, $a_0 = 0.1$, c = 0.58 and δ_t =0.001, corresponding to Problem 2.

tions. Two time integration schemes RK4 and TVD-RK3 are used. The method is stable, efficient and very easy in implementation. A large class of time-dependent nonlinear partial differential equation can be solved by this

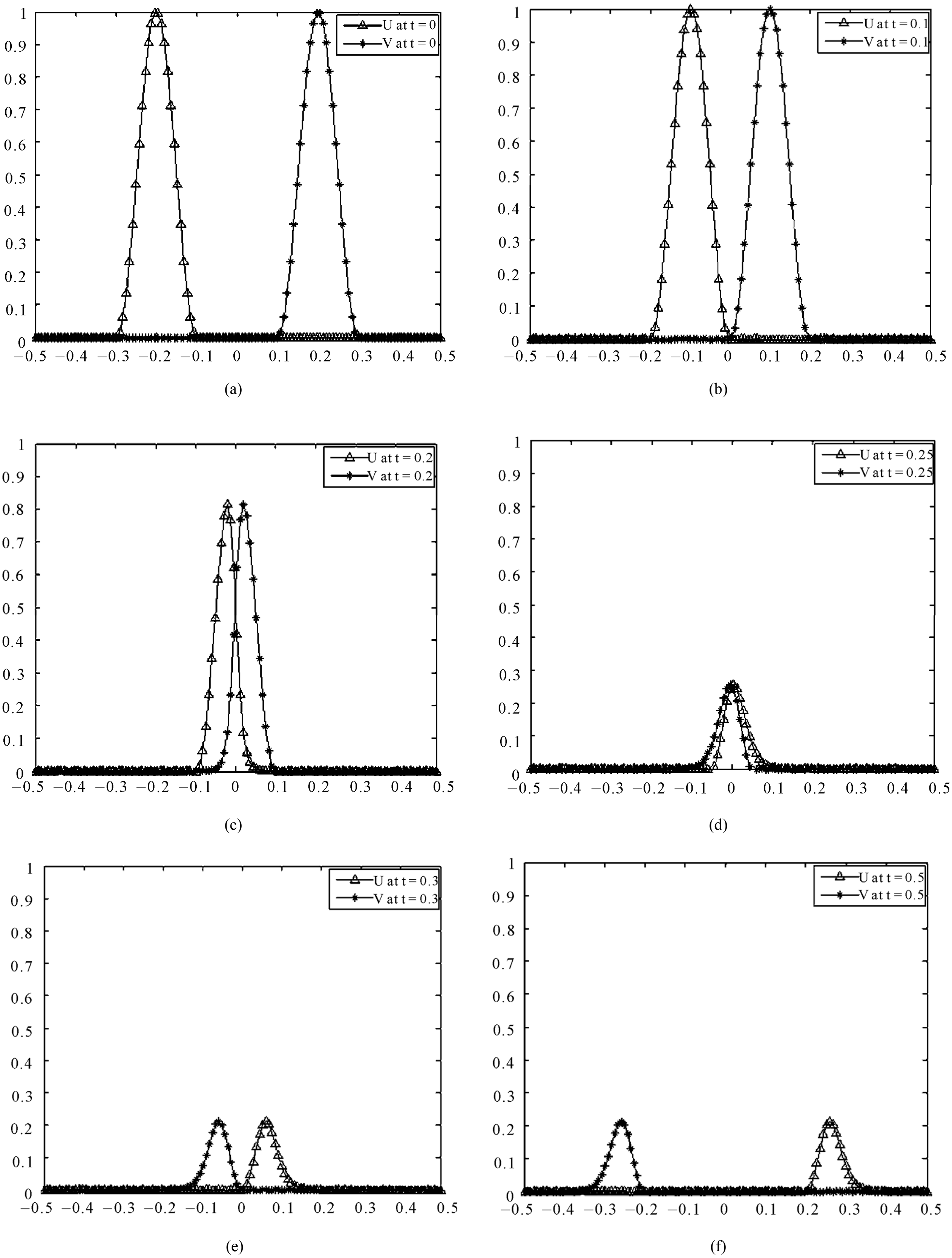

Figure 3. Numerical solution using quintics. Figures 3(*a*)-3(*f*) show the motion and interaction of the waves *u* and *v*.

technique.

5. Acknowledgements

The work presented in this paper is supported by HEC Pakistan through grants 063-281079-Ps3-169, IRSIP 14 Ps3.

6. References

[1] A. Osborne, "The Inverse Scattering Transform: Tools for the Nonlinear Fourier Analysis and Filtering of Ocean Surface Water Waves," *Chaos. Solitons & Fractals*, Vol. 5, No. 12, 1995, pp. 2623-37. doi:10.1016/0960-0779(94)E0118-9

[2] L. Ostrovsky and Y. A. Stepanyants, "Do Internal Solutions Exist in the Ocean," *Reviews of Geophysics*, Vol. 27, No. 3, 1989, pp. 293-310. doi:10.1029/RG027i003p00293

[3] G. C. Das and J. Sarma "Response to 'Comment on' a New Mathematical Approach for Finding the Solitary Waves in Dusty Plasma," *Physics of Plasmas*, Vol. 6, No. 11, 1999, pp. 4394-4397. doi:10.1063/1.873705

[4] R. Hirota and J. Satsuma, "Soliton Solutions of a Coupled Kortewege-de Vries Equation," *Physics Letters A*, Vol. 85, No. 8-9, 1981, pp. 407-408. doi:10.1016/0375-9601(81)90423-0

[5] Y. C. Hon and X. Z. Mao, "An Efficient Numerical Scheme for Burgers Equation," *Applied Mathematics and Computation*, Vol. 95, No. 1, 1998, pp. 37-50. doi:10.1016/S0096-3003(97)10060-1

[6] R. Chen and Z. Wu, "Solving Partial Differential Equation by Using Multiquadric Quasiinterpolation," *Applied Mathematics and Computation*, Vol. 186, No. 2, 2007, pp. 1502-1510. doi:10.1016/j.amc.2006.07.160

[7] D. Kaya and E. I. Inan, "Exact and Numerical Traveling Wave Solutions for Nonlinear Coupled Equations Using Symbolic Computation," *Applied Mathematics and Computation*, Vol. 151, No. 3, 2004, pp. 775-787. doi:10.1016/S0096-3003(03)00535-6

[8] Y. Xu, C.-W. Shu, "Local Discontinuous Galerkin Methods for the Kuramoto-Sivashinsky Equations and the Ito-Type Coupled Equations," *Computer Methods in Applied Mechanics and Engineering*, Vol. 195, No. 25-28, 2006, pp. 3430-3447. doi:10.1016/j.cma.2005.06.021

[9] L. M. B. Assas, "Variational Iteration Method for Solving Coupled-KdV Equations," *Chaos, Solitons & Fractals*, Vol. 38, No. 4, 2008, pp. 1225-1228. doi:10.1016/j.chaos.2007.02.012

[10] A. H. Khater, R. S. Temsah and M. M. Hassan, "A Chebyshev Spectral Collocation Method for Solving Burgers' Type Equations," *Journal of Computational and Applied Mathematics*, Vol. 222, No. 2, 2008, pp. 333-350. doi:10.1016/j.cam.2007.11.007

[11] M. Uddin, S. Haq and S. Islam, "Numerical Solution of Complex Modified Kortewegde Vries Equation by Mesh-Free Collocation Method," *Computers & Mathematics with Applications*, Vol. 58, No. 3, 2009, pp. 566-578. doi:10.1016/j.camwa.2009.03.104

[12] S. Islam, S. Haq and M. Uddin, "A Mesh Free Interpolation Method for the Numerical Solution of the Coupled Nonlinear Partial Differential Equations," *Engineering Analysis with Boundary Elements*, Vol. 33, No. 3, 2009, pp. 399-409.

[13] R. L. Hardy, "Multiquadric Equations of Topography and Other Irregular Surfaces," *Journal of Geophysical Research*, Vol. 76, No. 8, 1971, pp. 1905-1915. doi:10.1029/JB076i008p01905

[14] R. Franke, "Scattered Data Interpolation: Tests of Some Methods," *Mathematics of Computation*, Vol. 38, No. 157, 1982, pp. 181-200.

[15] R. Franke, "A Critical Comparison of Some Methods for Interpolation of Scattered Data," Technical Report NPS-53-79-003, Naval Postgraduate School, 1975.

[16] F. J. Hickernell and Y. C. Hon, "Radial Basis Function Approximation of the Surface Wind Field from Scattered Data," *International Journal of Applied Science and Computers*, Vol. 4, No. 3, 1998, pp. 221-247.

[17] M. A. Golberg, C. S. Chen and S. Karur, "Improved Multiquadric Apporoxmation for Partial Differential Equations," *Engineering Analysis with Boundary Elements*, Vol. 18, No. 1, 1996, pp. 9-17. doi:10.1016/S0955-7997(96)00033-1

[18] I. Babuska, U. Banerjee and J. E. Osborn, "Survey of Meshless and Generalized Finite Element Methods: A Unified Approach," *Acta Numerica*, Vol. 12, 2003, pp. 1-125. doi:10.1017/S0962492902000090

[19] D. Brown, L. Ling, E. Kansa and J. Levesley, "On Approximate Cardinal Preconditioning Methods for Solving PDEs with Radial Basis Functions," *Engineering Analysis with Boundary Elements*, Vol. 29, No. 4, 2005, pp. 343-353. doi:10.1016/j.enganabound.2004.05.006

[20] G. E. Fasshauer, A. Q. M. Khaliq and D. A. Voss, "Using Meshfree Approximation for Multi-Asset American Option Problems," *Journal of the Chinese Institute of Eng*, Vol. 27, No. 4, 2004, pp. 563-571. doi:10.1080/02533839.2004.9670904

[21] B. Fornberg, E. Larsson and G. Wright, "A New Class of Oscillatory Radial Basis Functions," *Computers & Mathematics with Applications*, Vol. 51, No. 8, 2006, pp. 1209-1222. doi:10.1016/j.camwa.2006.04.004

[22] E. J. Kansa and Y. C. Hon, "Circumventing the Illconditioning Problem with Multiquadric Radial Basis Functions: Applications to Elliptic Partial Differential Equations," *Computers & Mathematics with Applications*, Vol. 39, No. 7-8, 2000, pp. 123-137. doi:10.1016/S0898-1221(00)00071-7

[23] I. Dag and Y. Dereli, "Numerical Solutions of KdV Equation Using Radial Basis Functions," *Applied Mathematical Modelling*, Vol. 32, No. 4, 2008, pp. 535-546. doi:10.1016/j.apm.2007.02.001

[24] M. Dehghan and M. Tatari, "Determination of a Control Parameter in a One-Dimensional Parabolic Equation Us-

ing the Method of Radial Basis Functions," *Mathematical and Computer Modelling*, Vol. 44, No. 11-12, 2006, pp. 1160-1168. doi:10.1016/j.mcm.2006.04.003

[25] M. Uddin, S. Haq and S. Islam, "A Mesh-Free Numerical Method for Solution of the Family of Kuramoto-Sivashinsky Equations," *Applied Mathematics and Computation*, Vol. 212, No. 2, 2009, pp. 458-469. doi:10.1016/j.amc.2009.02.037

[26] W. E. Schiesser, "The Numerical Method of Lines: Integration of Partial Differential Equations," Academic Press, San Diego, 1991.

[27] Q. Shen, "A Meshless Method of Lines for the Numerical Solution of KdV Equation Using Radial Basis Functions," *Engineering Analysis with Boundary Elements*, Vol. 33, No. 10, 2009, pp. 1171-1180. doi:10.1016/j.enganabound.2009.04.008

[28] S. Gottlieb and C. W. Shu, "Total Variation Diminishing Runge-Kutta Schemes," *Mathematics of Computation*, Vol. 67, No. 221, 1998, pp. 73-85. doi:10.1090/S0025-5718-98-00913-2

[29] R. Hirota and J. Satsuma, "A Coupled KdV Equation is One Case of the Four-Reduction of the KP Hierarchy," *Journal of the Physical Society of Japan*, Vol. 51, No. 10, 1982, pp. 3390-3397. doi:10.1143/JPSJ.51.3390

